© 2017. Published by The Company of Biologists Ltd | Journal of Cell Science (2017) 130, 577-589 doi:10.1242/jcs.191213

RESEARCH ARTICLE

Multiple routes of endocytic internalization of PDGFRβ contribute to PDGF-induced STAT3 signaling

Kamil Jastrzębski[1], Daria Zdżalik-Bielecka[1], Agnieszka Mamińska[1], Yannis Kalaidzidis[2], Carina Hellberg[3,*] and Marta Miaczynska[1,‡]

ABSTRACT

Platelet-derived growth factor receptor β (PDGFRβ) is a receptor tyrosine kinase which upon activation by PDGF-BB stimulates cell proliferation, migration and angiogenesis. Ligand binding induces intracellular signaling cascades but also internalization of the receptor, eventually resulting in its lysosomal degradation. However, endocytic trafficking of receptors often modulates their downstream signaling. We previously reported that internalization of PDGFRβ occurs via dynamin-dependent and -independent pathways but their further molecular determinants remained unknown. Here we show that, in human fibroblasts expressing endogenous PDGFRβ and stimulated with 50 ng/ml PDGF-BB, ligand–receptor uptake proceeds via the parallel routes of clathrin-mediated endocytosis (CME) and clathrin-independent endocytosis (CIE). CME involves the canonical AP2 complex as a clathrin adaptor, while CIE requires RhoA–ROCK, Cdc42 and galectin-3, the latter indicating lectin-mediated internalization via clathrin-independent carriers (CLICs). Although different uptake routes appear to be partly interdependent, they cannot fully substitute for each other. Strikingly, inhibition of any internalization mechanism impaired activation of STAT3 but not of other downstream effectors of PDGFRβ. Our data indicate that multiple routes of internalization of PDGFRβ contribute to a transcriptional and mitogenic response of cells to PDGF.

KEY WORDS: Platelet-derived growth factor receptor β, PDGFRβ, Platelet-derived growth factor BB, PDGF-BB, Endocytosis, Signal transducer and activator of transcription 3, STAT3, Rho GTPase

INTRODUCTION

Ligand-activated receptor tyrosine kinases (RTKs) can be internalized by distinct pathways of endocytosis (Goh and Sorkin, 2013). To date, the best-defined entry portal into mammalian cells is clathrin-mediated endocytosis (CME). Within this route, cargo selected for internalization interacts with adaptor proteins, such as the heterotetrameric AP2 complex, and is included into forming clathrin-coated pits. Subsequent scission of nascent vesicles is performed by the large GTPase dynamin (McMahon and Boucrot, 2011). In parallel, numerous pathways of clathrin-independent endocytosis (CIE) have been described. Although their exact classification is still a matter of debate, their common denominator is the involvement of actin cytoskeleton and Rho GTPases (Lamaze et al., 2001; Grassart et al., 2008; Lundmark et al., 2008; Doherty and McMahon, 2009; Mayor et al., 2014). In addition, cholesterol- and glycosphingolipid-dependent formation of plasma membrane domains is important for CIE, which may involve extracellular lectins to cluster cargo destined for internalization (Johannes et al., 2015). Dynamin can mediate scission of some clathrin-free endocytic intermediates, but other CIE pathways are independent of its activity (Mayor et al., 2014). Regardless of entry route (CME or CIE), internalized RTKs are generally sorted to early endosomes from where they are either recycled back to the plasma membrane or targeted for degradation in lysosomes (Goh and Sorkin, 2013).

Endocytic trafficking of a given RTK can impinge upon its signal transduction in multiple ways. Firstly, the pathway and kinetics of receptor internalization may modulate its signaling activity. Secondly, the sorting to degradation or recycling determines the balance between termination and sustenance of signaling, respectively. Thirdly, compartmentalization of a receptor in different endosomal organelles may diversify its signaling output in time and space (Gonnord et al., 2012; Sigismund et al., 2012; Miaczynska, 2013; Irannejad et al., 2015; Villaseñor et al., 2016). Still, for most RTKs, the routes of endocytic trafficking and their impact on signaling remain poorly investigated.

Platelet-derived growth factor receptor β (PDGFRβ) is a RTK activated *in vivo* primarily by platelet-derived growth factor BB (PDGF-BB), which is a disulfide bond-linked homodimer of two PDGF-B polypeptides. PDGFRβ activation induces cell proliferation, migration and angiogenesis (Heldin and Westermark, 1999; Andrae et al., 2008). Ligand binding, dimerization and autophosphorylation of PDGFRβ initiates signaling pathways that involve, among other proteins, AKT proteins, extracellular signal-regulated kinase (ERK) proteins, glycogen synthase kinase 3β (GSK3β), phospholipase Cγ (PLCγ) and signal transducer and activator of transcription (STAT) proteins (Heldin and Westermark, 1999). Moreover, ligand binding causes internalization and eventually lysosomal degradation of the receptor (Nilsson et al., 1983). Importantly, PDGFRβ bound to PDGF-BB remains active following internalization and may thus continue signaling from endosomes (Wang et al., 2004).

Initially, PDGFRβ was described to follow CME for its internalization (Nilsson et al., 1983; Kapeller et al., 1993), although more recent reports also indicate a possible engagement of clathrin-independent mechanisms (De Donatis et al., 2008; Boucrot et al., 2015). However, the regulators and significance of PDGFRβ uptake by CIE remained unknown. We previously demonstrated that PDGF-BB can be internalized via dynamin-dependent and -independent pathways, with dynamin activity being crucial for STAT3 activation to initiate cell proliferation (Sadowski et al., 2013). Here, we further characterize endocytic transport of PDGFRβ in human fibroblasts and identify its molecular mediators. We demonstrate that CIE of PDGFRβ requires the actin

[1]Laboratory of Cell Biology, International Institute of Molecular and Cell Biology, Warsaw 02-109, Poland. [2]Max Planck Institute of Molecular Cell Biology and Genetics, Dresden 01307, Germany. [3]School of Biosciences, University of Birmingham, Birmingham B15 2TT, UK.
*Deceased

‡Author for correspondence (miaczynska@iimcb.gov.pl)

M.M., 0000-0003-0031-5267

Received 4 May 2016; Accepted 5 December 2016

Journal of Cell Science (2017) 130, 577-589 doi:10.1242/jcs.191213

cytoskeleton, RhoA–ROCK, Cdc42 and galectin-3. However, independently of the route of internalization, intracellular accumulation of PDGFRβ is necessary to fully activate STAT3 and induce expression of several PDGF target genes. These data argue that sustained STAT3 signaling from endosomal compartments contributes to the mitogenic response to PDGF.

RESULTS

PDGFRβ is partly internalized by clathrin-dependent endocytosis which is required for STAT3 activation

Our previous data demonstrated that internalization of ligand-stimulated PDGFRβ in human fibroblasts was impaired but not completely blocked in the presence of dynamin inhibitors (Sadowski et al., 2013). This suggested that multiple pathways of endocytosis are responsible for PDGF-BB uptake. To extend these findings, we analyzed to what degree PDGFR endocytosis involved the classical regulators of CME, such as AP2 and clathrin heavy chain (CHC, also known as CLTC). We used two independent siRNA sequences to deplete a μ2 subunit of the AP2 complex (AP2μ2, also known as AP2M1) or CHC in CCD-1070Sk human skin fibroblasts, which express high levels of endogenous PDGFRβ. In parallel, we also knocked down dynamin 2 (DNM2), to compare the effects of its depletion to the previously reported usage of dynamin inhibitors (Sadowski et al., 2013). Knockdown efficiencies of AP2μ2, CHC or DNM2 were verified by western blotting (Fig. S1A–C). Importantly, depletion of these proteins did not affect basal levels of PDGFRβ protein (Fig. S1A–C). Unless otherwise indicated, to quantify internalization of the receptor, cells were stimulated with PDGF-BB (50 ng/ml) and fluorescently labeled transferrin (25 μg/ml) for up to 30 min, fixed, stained for PDGFRβ and imaged. Confocal images were quantitatively analyzed using MotionTracking software (Collinet et al., 2010) to measure endosomal accumulation of PDGFRβ and transferrin, the latter reflecting the activity of CME.

Depletion of AP2μ2, CHC or DNM2 inhibited endocytosis of PDGFRβ on average by ∼50% after 30 min of stimulation (Fig. 1A, C,E; Table S1), observed consistently with all small interfering RNA (siRNA) oligonucleotides used. As expected, the inhibition of transferrin uptake in these cells was stronger, reaching 70-95% (Fig. 1B,D,F; Table S1). Knockdown of AP2μ2 was the most potent in reducing internalization of transferrin, possibly due to its more efficient depletion as compared to CHC or DNM2 (Fig. S1A–C). Still, under the condition of an almost complete block of transferrin uptake (>95% for siRNA AP2M1_1), internalization of PDGFRβ was moderately decreased by only ∼50% (Fig. 1A,B; Table S1). These data confirm that clathrin- and AP2-driven endocytosis partially mediates uptake of PDGFRβ when stimulated by 50 ng/ml PDGF-BB, which represents a ligand dose that induces cell proliferation (Sadowski et al., 2013). These results further suggest that under these conditions, clathrin-independent pathways must operate in parallel to CME to ensure complete internalization of PDGFRβ. Moreover, the effects of DNM2 depletion closely resemble the previously reported effects of dynamin inhibitors on PDGFRβ endocytosis (Sadowski et al., 2013). The involvement of dynamin may reflect both its well-documented action in CME and in clathrin-independent but dynamin-dependent routes of PDGFRβ internalization.

Studies of endocytosis of epidermal growth factor receptor (EGFR) indicate that ligand concentration may affect the internalization route (Sigismund et al., 2005, 2008). Specifically, low doses of EGF induce predominantly CME, while both CME and CIE are employed for EGF uptake at higher concentrations. In our experimental model, 10 ng/ml PDGF-BB was the lowest dose that induced quantifiable receptor internalization (Fig. S1D). We therefore tested effects of depletion of AP2μ2, CHC or DNM2 on PDGFRβ internalization induced by 10 ng/ml PDGF-BB. Receptor uptake under these conditions was strongly inhibited (by 77–93% after 15 min of ligand addition; Fig. S1E; Table S2), with transferrin internalization blocked to a similar extent (82–95% inhibition; Fig. S1F). These data confirm that, by analogy to EGFR, endocytosis of PDGFRβ stimulated by lower doses of PDGF-BB occurs predominantly by CME.

We further measured whether knockdown of CME components affected signal transduction downstream of ligand-stimulated PDGFRβ. To this end, we employed a higher (50 ng/ml) dose of PDGF, as lower concentrations of the ligand do not activate STAT3 (Sadowski et al., 2013). We observed that depletion of AP2μ2 and DNM2 reduced STAT3 phosphorylation induced by 50 ng/ml PDGF-BB (Fig. 1G–I). Moreover, two out of three siRNAs against CHC also diminished STAT3 activation by PDGF-BB (Fig. 1H; Fig. S1I). In all these cases activation of PDGFRβ itself, AKT, PLCγ or GSK3β remained unchanged (Fig. S1G–J). ERK1 and ERK2 (ERK1/2, also known as MAPK3 and MAPK1, respectively) kinases were not analyzed because they are constitutively active in CCD-1070Sk cells and not further activated by PDGF-BB (Sadowski et al., 2013). Taken together, these data indicate that clathrin- and dynamin-mediated internalization of PDGFRβ is required specifically for full activation of STAT3 but not of other effectors of PDGF-BB signaling.

Clathrin-independent endocytosis of PDGFRβ is mediated by RhoA but not Rac1

To further verify involvement of clathrin-independent pathways in PDGFRβ internalization, we tested the effect of perturbation of actin cytoskeleton, a common denominator of several CIE routes, on PDGFRβ uptake. We thus analyzed internalization of PDGFRβ in cells treated with latrunculin A, an inhibitor of actin polymerization. Indeed, PDGFRβ endocytosis was reduced by ∼30% as compared to DMSO-treated cells at 15–20 min of PDGF-BB stimulation, while uptake of transferrin was unperturbed (Fig. S2A,B; Table S3). These results suggested that actin-mediated, clathrin-independent endocytic pathways participate in internalization of PDGFRβ. Uptake via caveolae represents one of the CIE routes (Mayor et al., 2014). However, we determined that colocalization between PDGFRβ and caveolin-1 was very limited in CCD-1070Sk cells (data not shown); thus, caveolae were unlikely to account for the internalization of substantial amounts of the receptor.

The Rho family of small G proteins regulates various aspects of actin dynamics in the cell. Moreover, Rac1, RhoA and Cdc42 have been reported to participate in different pathways of CIE (Mayor et al., 2014). We thus systematically investigated how interference with the levels and/or activity of these proteins affected PDGFRβ internalization. To this end, we applied overexpression of GFP-tagged dominant-active or dominant-negative mutants of Rac1, RhoA and Cdc42, as well as their chemical inhibition and siRNA-mediated depletion.

With regard to Rac1, we did not observe any noticeable changes in PDGFRβ endocytosis in cells expressing constitutively active (Q61L) or inactive (T17N) Rac1 mutants (Fig. S2C). Inhibition of Rac1 activity with the NSC23766 compound (Akbar et al., 2006) did not affect PDGFRβ internalization (Fig. S2D), although it moderately reduced transferrin uptake (Fig. S2E). Furthermore, NSC23766 did not alter PDGF-induced STAT3 activation (Fig. S2F). These data argue against involvement of Rac1 in endocytosis and signaling of PDGFRβ.

Expression of RhoA mutants affected the endocytic trafficking of PDGFRβ (Fig. 2A). The presence of constitutively active (Q63L)

Journal of Cell Science

Journal of Cell Science (2017) 130, 577-589 doi:10.1242/jcs.191213

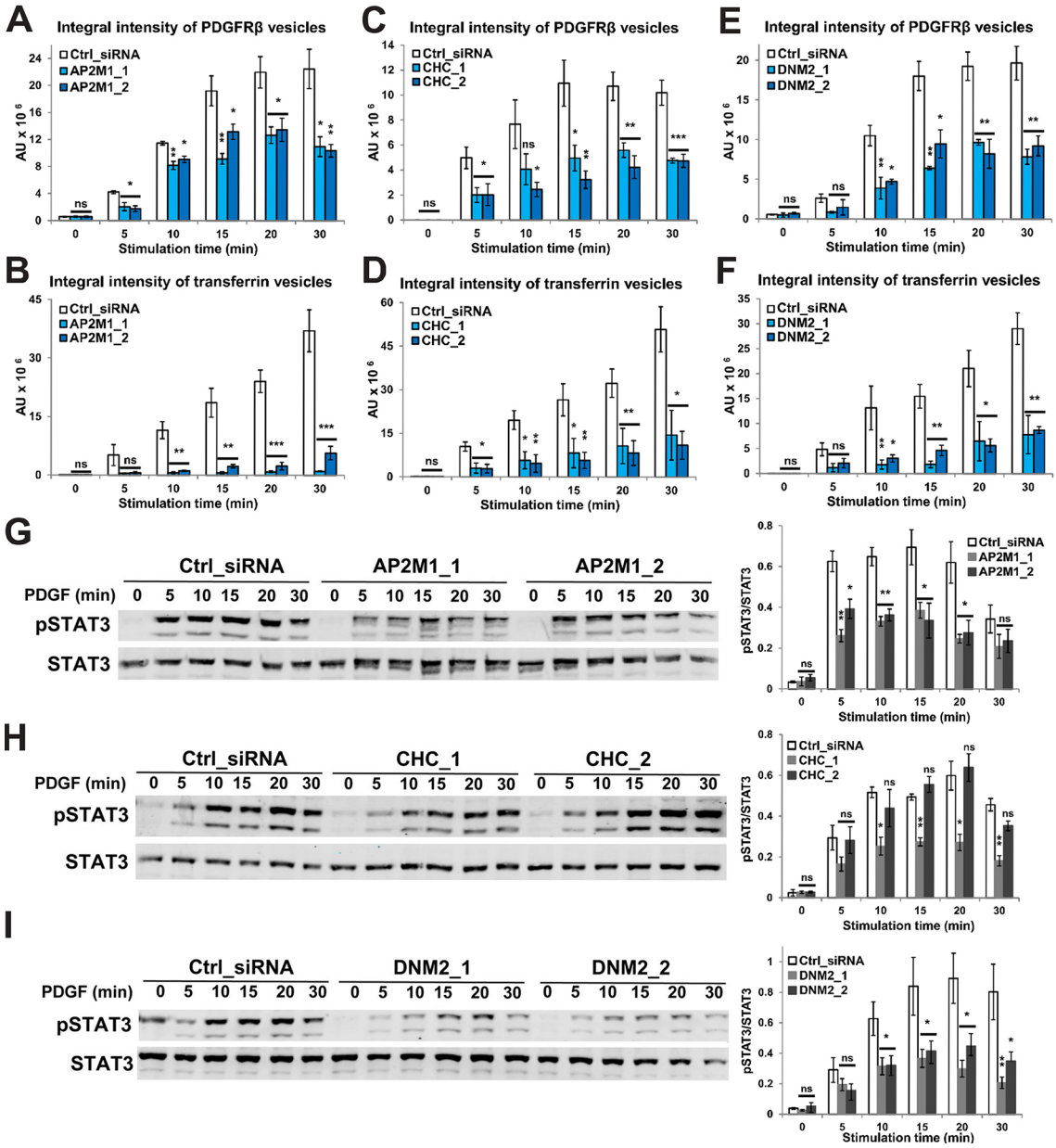

Fig. 1. PDGFRβ internalization and signaling depend on AP2, clathrin and dynamin 2. (A–F) PDGFRβ is internalized by CME. Immunofluorescence analysis was performed upon silencing of AP2μ2 (AP2M1; A,B), CHC (C,D) or DNM2 (E,F) with two siRNAs (30 nM, numbered _1 or _2) or in control siRNA-transfected cells (Ctrl_siRNA). Cells were stimulated with PDGF-BB and transferrin. Integral fluorescence intensities of PDGFRβ- (A,C,E) or transferrin-positive vesicles (B,D,F) were quantified. (G–I) PDGF-induced STAT3 phosphorylation depends on AP2, clathrin and dynamin 2. STAT3 phosphorylation and total abundance were detected by western blotting in lysates of cells depleted of AP2μ2 (G), CHC (H) or DNM2 (I) with two siRNAs (as above) or in control siRNA-transfected cells, and stimulated with PDGF-BB. Band intensities were measured and phosphorylated STAT3 (pSTAT3) abundance normalized to total STAT3 abundance (graphs). Data represent mean±s.e.m. of three (A,B,E–H), four (C,D) or six (I) independent experiments. ns, not significant; *$P \leq 0.05$, **$P \leq 0.01$, ***$P \leq 0.001$ versus control (one-way ANOVA and Dunnett's test).

RhoA caused prolonged peripheral accumulation of PDGFRβ-containing endosomes. As shown in Fig. 2A, at 20 min of PDGF-BB treatment, endosomes harboring PDGFRβ and EEA1 were distributed throughout the cytoplasm of control cells. In RhoA-Q63L expressing cells, these endosomes were enriched in the vicinity of the plasma membrane, suggesting a possible defect in trafficking of the ligand–receptor complexes. Moreover, cells expressing an inactive RhoA-T19N mutant exhibited lower intracellular accumulation of PDGFRβ, without major changes in the morphology or localization of early endosomes stained with EEA1 (Fig. 2A). These observations suggested that RhoA may be potentially involved in PDGFRβ endocytosis. To further verify these data, cells were treated with agents blocking the RhoA function: C3 toxin and Rhosin (Narumiya et al., 1988; Shang et al., 2012). Both inhibitors interfered with the uptake of PDGFRβ. The amounts of internalized PDGFRβ after 15 min of PDGF-BB treatment were reduced by 37±6% by C3 toxin and by 40±8% by Rhosin (mean±s.e.m.), with a similar degree of inhibition observed for up to 30 min (Fig. 2B; Table S3). Transferrin endocytosis was not significantly affected under these conditions (Fig. 2C; Table S3). Cumulatively, these results suggested an involvement of RhoA but not Rac1 in the uptake of PDGFRβ.

Journal of Cell Science (2017) 130, 577-589 doi:10.1242/jcs.191213

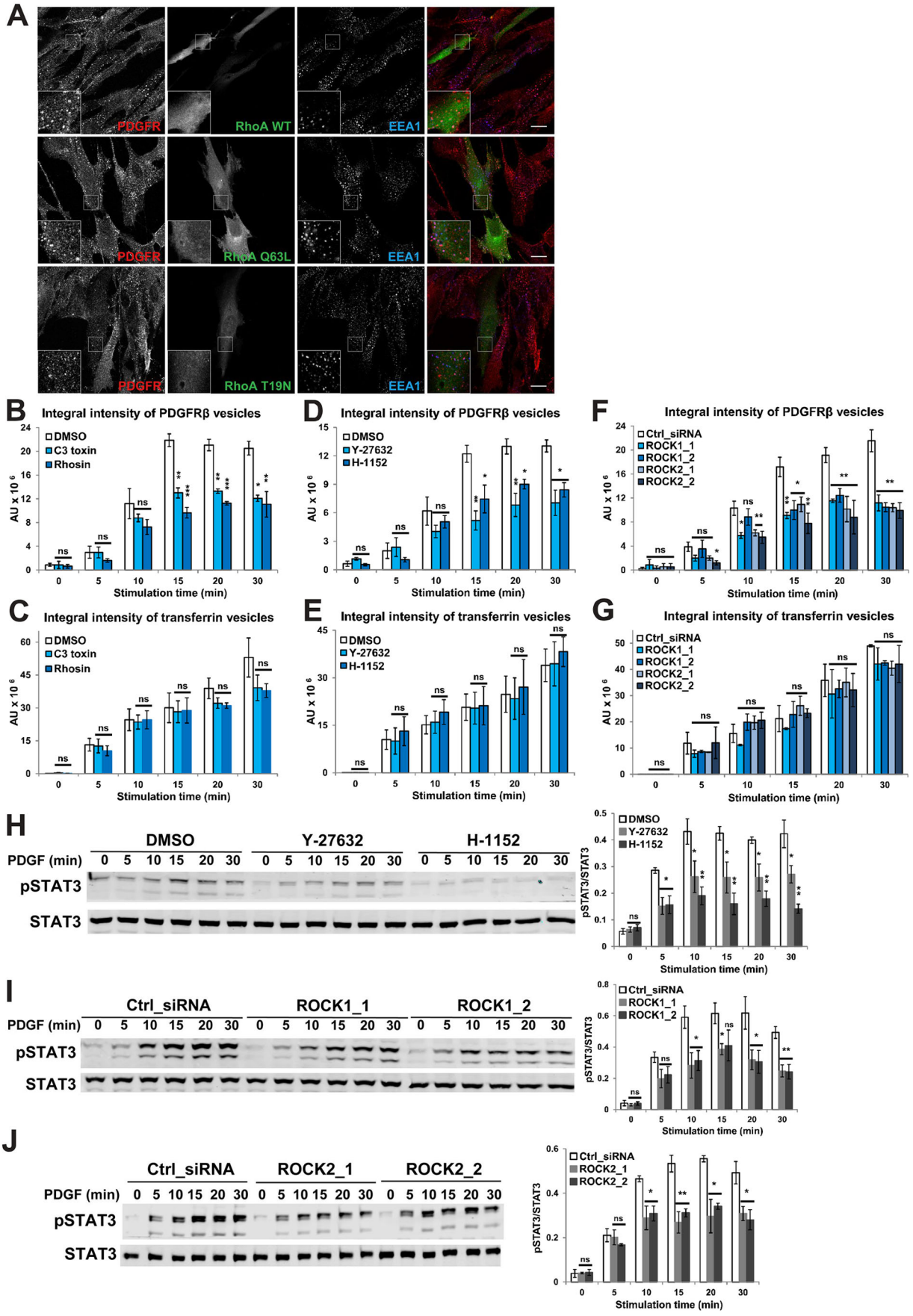

Fig. 2. See next page for legend.

Journal of Cell Science

Journal of Cell Science (2017) 130, 577-589 doi:10.1242/jcs.191213

Fig. 2. RhoA and ROCK1/2 activities are required for PDGFRβ internalization and PDGF-dependent signaling. (A–G) RhoA and ROCK1/2 activities contribute to PDGFRβ internalization. (A) Immunofluorescence analysis for PDGFRβ (red) and EEA1 (blue) was performed upon overexpression of GFP-tagged RhoA wild-type (WT), RhoA-Q63L or RhoA-T19N (green), after stimulation with PDGF-BB for 20 min. Scale bars: 20 µm. (B–G) Immunofluorescence analysis was performed after pretreatment with the RhoA inhibitors C3 toxin or Rhosin for 16 h (B,C), ROCK1/2 inhibitors Y-27632 or H-1152 for 30 min (D,E) or with DMSO, and stimulation with PDGF-BB and transferrin. Alternatively, cells were depleted of ROCK1 or ROCK2 with two siRNAs (10 nM, numbered _1 or _2) or transfected with control siRNA (Ctrl_siRNA) (F,G) and stimulated with PDGF-BB and transferrin for the indicated times. Integral fluorescence intensities of PDGFRβ- (B,D,F) or transferrin-positive vesicles (C,E,G) were quantified. (H–J) PDGF-induced STAT3 phosphorylation depends on ROCK1/2 activities. STAT3 phosphorylation and total abundance were detected by western blotting in lysates of cells pretreated with Y-27632 or H-1152 or DMSO for 30 min (H), or in cells depleted of ROCK1 (I) or ROCK2 (J) with two siRNAs (as above) or transfected with control siRNA, and stimulated with PDGF-BB. Band intensities were measured and phosphorylated STAT3 (pSTAT3) abundance normalized to total STAT3 abundance (H–J, graphs). Data represent mean± s.e.m. of three (B–G,J) or four (H–I) independent experiments. ns, not significant; *$P\leq0.05$, **$P\leq0.01$, ***$P\leq0.001$ versus control (one-way ANOVA and Dunnett's test).

RhoA- and ROCK-mediated CIE of PDGFRβ is necessary for PDGF-induced activation of STAT3

Among key RhoA effectors are the Rho-dependent kinases ROCK1 and ROCK2 (Riento and Ridley, 2003). To verify whether ROCK1 and ROCK2 (hereafter ROCK1/2) are involved in PDGFRβ internalization, we applied their two ATP-competitive, selective inhibitors Y-27632 and H-1152 (Uehata et al., 1997; Tamura et al., 2005). Treatment of cells with both compounds reduced PDGFRβ endocytosis without affecting transferrin internalization (Fig. 2D,E). Specifically, at 15 min after ligand addition, PDGFRβ internalization was decreased by 58±5% and 38±14% (mean±s.e.m.) by Y-27632 and H-1152, respectively, as compared to control (Fig. 2D; Table S3). To confirm the data obtained with ROCK inhibitors, internalization of PDGFRβ and transferrin was monitored after siRNA-mediated knockdown of ROCK1 or ROCK2. Depletion of these proteins did not affect basal levels of PDGFRβ protein (Fig. S3A,B) or endocytosis of transferrin (Fig. 2G; Table S3). However, cells with silenced expression of *ROCK1* or *ROCK2* showed decreased amounts of internalized PDGFRβ (Fig. 2F; Table S3), with a range similar to cells treated with ROCK inhibitors (reduction of 35–55% for individual siRNA oligonucleotides at 15 min after PDGF-BB addition). Cumulatively, these data established that interfering with the function of RhoA or ROCK1/2 impaired uptake of PDGF but not transferrin internalized by CME. We therefore conclude that RhoA and ROCK1/2 are involved in CIE of PDGFRβ.

We further analyzed whether interference with the function of ROCK1/2 affected PDGF-induced signaling. Pharmacological inhibition or depletion of ROCK1 or ROCK2 impaired activation of STAT3 (Fig. 2H–J) but not activation of AKT proteins, GSK3β, PLCγ or PDGFRβ itself (Fig. S3C–E). A similar pattern of signaling was observed upon inhibition of CME (Fig. 1G,H and Fig. S1G–I), suggesting that full STAT3 activation requires internalization of PDGFRβ, and that this is independent of the specific uptake pathway.

Cdc42 is required for clathrin-independent internalization of PDGFRβ and PDGF-induced activation of STAT3

To test a possible involvement of Cdc42 in PDGFRβ endocytosis, we analyzed how expression of Cdc42 mutants affected ligand-induced PDGFRβ trafficking. In cells overexpressing a constitutively active Cdc42-Q61L mutant, PDGFRβ- and EEA1-positive vesicles were enlarged and localized close to the plasma membrane even at 20 min after PDGF addition, while at this time point the receptor localized in the perinuclear region in control cells (Fig. 3A). In contrast, cells expressing an inactive Cdc42-T17N mutant exhibited a decreased number of PDGFRβ-positive endosomes, with no visible changes in the number or distribution of early endosomes marked with EEA1 (Fig. 3A). These data suggested a possible involvement of Cdc42 in endocytosis of PDGFRβ.

As the next step, we treated cells with ML141, a selective, non-competitive inhibitor of Cdc42 (Surviladze et al., 2010). This treatment decreased PDGFRβ internalization without affecting transferrin uptake (Fig. 3B,C). At 15 min, Cdc42 inhibitor reduced PDGFRβ endocytosis by 56±6% (mean±s.e.m.) compared to cells treated with DMSO as a solvent control (Table S4). However, the inhibitory effect of ML141 on PDGFRβ internalization was no longer significant at 30 min after addition of the ligand (Fig. 3B; Table S4), suggesting a possible compensatory mechanism of uptake.

To confirm a role of Cdc42 in PDGFRβ endocytosis, *CDC42* expression was silenced by RNA interference (RNAi). Depletion of Cdc42 did not affect levels of PDGFRβ (Fig. S4A) but impaired its endocytosis by ∼45% at 15 min after addition of the ligand (Fig. 3D; Table S4). In contrast to ML141 treatment, this degree of inhibition persisted at later time points (30 min after ligand addition; Fig. 3D; Table S4). Importantly, Cdc42 knockdown did not alter transferrin internalization (Fig. 3E; Table S4). These data indicate that Cdc42 is involved in CIE of PDGFRβ, as with RhoA and ROCK1/2.

We then investigated how perturbation of PDGFRβ endocytosis by ML141 or Cdc42 depletion correlated with PDGF-induced signaling. Consistently, both regimes reduced PDGF-dependent STAT3 phosphorylation (Fig. 3F,G), without affecting the other components of PDGFRβ signaling (Fig. S4B,C). These results reinforce our conclusion about the requirement of PDGFRβ internalization for full activation of STAT3.

Components of the CLIC and GEEC pathway, CD44 and galectin-3, take part in PDGFRβ internalization

Specific involvement of RhoA and Cdc42 in uptake of PDGFRβ but not transferrin provided evidence for CIE of the receptor. We verified whether PDGFRβ colocalized with known, widely expressed cargo molecules taken up by this mode of internalization, such as CD44 and CD98 (a heterodimer of SLC3A2 and SLC7A5) (Eyster et al., 2009). Endocytosis of these proteins can be stimulated by antibodies targeting their extracellular portions (Eyster et al., 2009). We observed a 30% colocalization between ligand-stimulated PDGFRβ and internalized CD44, starting from 10 min after addition of PDGF-BB and anti-CD44 antibody (Fig. 4A,B). In contrast, the percentage of colocalization between vesicles harboring PDGFRβ and CD98 was below 10% (Fig. 4A,B). In addition, CD44 colocalization with transferrin was below 10% until 10 min of internalization (Fig. 4C), suggesting that CD44 traffics through a different intermediate compartment to transferrin. After 15 min, CD44 colocalized more extensively with transferrin (>40%), which could reflect its recycling back to plasma membrane via classical recycling endosomes along with transferrin receptor. In contrast, CD98 colocalized more extensively with transferrin even at early time points (above 20% at 10 min; Fig. 4C).

CD44 acts as a hyaluronan receptor, and is reported to interact with a number of signaling receptors, including PDGFRβ (Lakshminarayan et al., 2014; Porsch et al., 2014). CIE of CD44 occurs via clathrin-independent carriers (CLICs) (Eyster et al.,

Journal of Cell Science (2017) 130, 577-589 doi:10.1242/jcs.191213

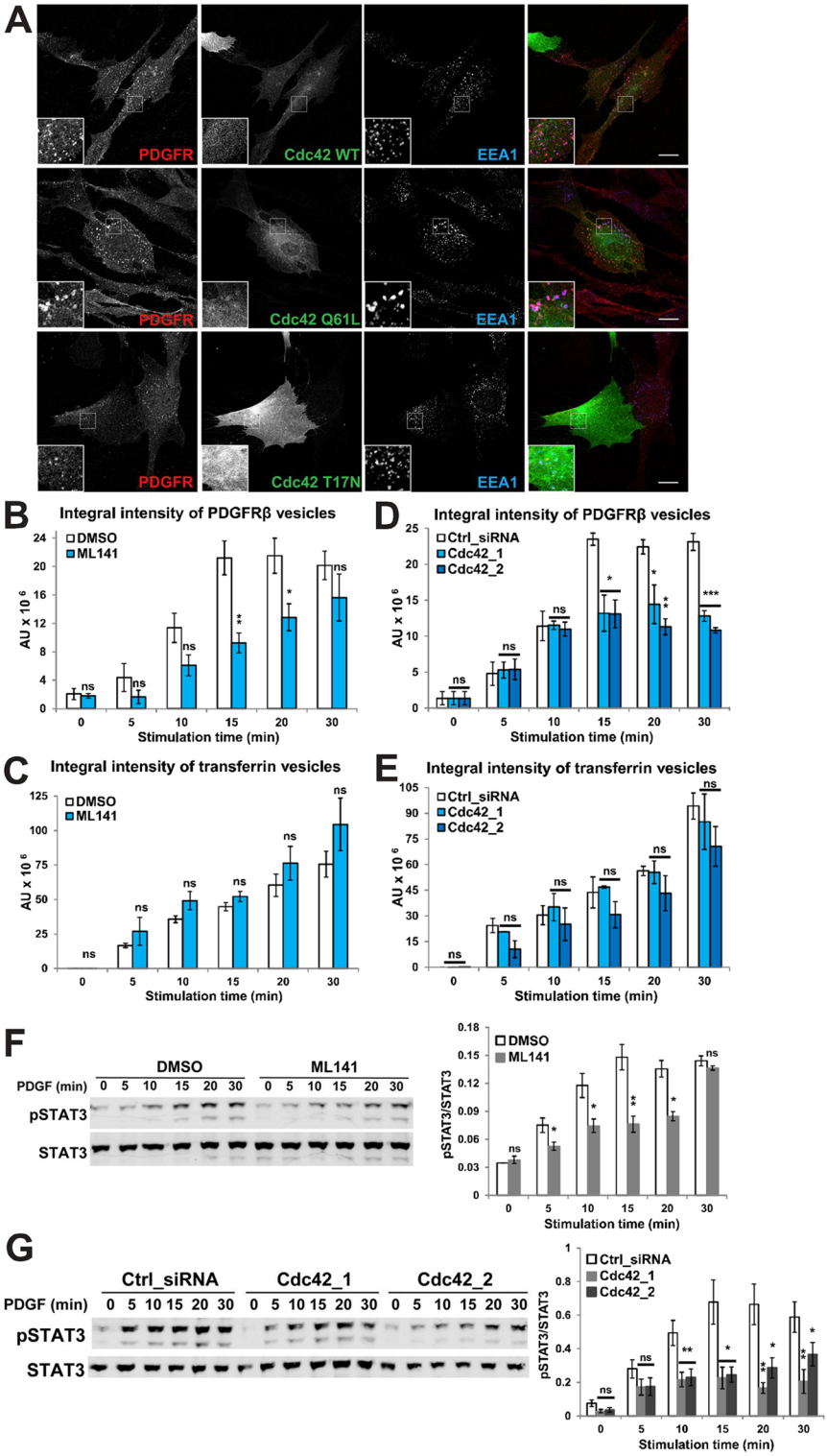

Fig. 3. Cdc42 activity is necessary for PDGFRβ internalization and PDGF-dependent signaling. (A–E) Inhibition or depletion of Cdc42 affects PDGFRβ internalization. (A) Immunofluorescence analysis for PDGFRβ (red) and EEA1 (blue) was performed upon overexpression of GFP-tagged Cdc42 wild-type (WT), Cdc42-Q61L or Cdc42-T17N (green) and stimulation with PDGF-BB for 20 min. Scale bars: 20 µm. (B–E) Immunofluorescence analysis was performed in cells pretreated with Cdc42 inhibitor ML141 or DMSO for 30 min (B,C) or depleted of Cdc42 with two siRNAs (10 nM, numbered _1 or _2) or transfected with control siRNA (Ctrl_siRNA) (D,E), and stimulated with PDGF-BB and transferrin. Integral fluorescence intensities of PDGFRβ- (B,D) or transferrin-positive vesicles (C,E) were quantified. (F,G) PDGF-induced STAT3 phosphorylation depends on Cdc42 activity. STAT3 phosphorylation and total abundance were detected by western blotting in lysates of cells pretreated with ML141 or DMSO for 30 min (F) or in cells depleted of Cdc42 (G) with two siRNAs (as above) or transfected with control siRNA and stimulated with PDGF-BB. Band intensities were measured and phosphorylated STAT3 (pSTAT3) abundance normalized to total STAT3 abundance (F,G, graphs). Data represent mean±s.e.m. of five (B,C), three (D,E,G) or four (F) independent experiments. ns, not significant; *$P \leq 0.05$, **$P \leq 0.01$, ***$P \leq 0.001$ versus respective control time points [one-way ANOVA and Dunnett's test (D,E,G) or Student's *t*-test (B,C,F)].

2009; Howes et al., 2010) and is mediated by galectin-3 (Lakshminarayan et al., 2014). We thus verified whether CD44 and galectin-3 are required for uptake of PDGFRβ. Knockdown of CD44 (Fig. S4D) impaired both internalization of PDGFRβ and transferrin (Fig. 4D,E; Table S5), although an inhibition of PDGFRβ uptake was more pronounced (63% versus 30% for siRNA CD44_1, and 53% versus 30% for siRNA CD44_2 at 30 min after addition of the ligand). Of two siRNA targeting galectin-3 (GAL3_1, GAL3_2), one (GAL3_1) caused a marked changes in morphology of cells (data not shown) and was excluded from further analysis. Depletion of galectin-3 using the other siRNA oligonucleotide (GAL3_2) decreased the amounts of internalized PDGFRβ without affecting transferrin endocytosis (Fig. 4F,G; Fig. S4E, Table S5). The involvement of galectin-3 in PDGFRβ endocytosis was confirmed by its depletion using two further siRNA oligonucleotides from another supplier (GAL3_3 and GAL3_4, Dharmacon; Fig. S4F) which reduced PDGFRβ internalization to a comparable extent to that observed for

Journal of Cell Science (2017) 130, 577-589 doi:10.1242/jcs.191213

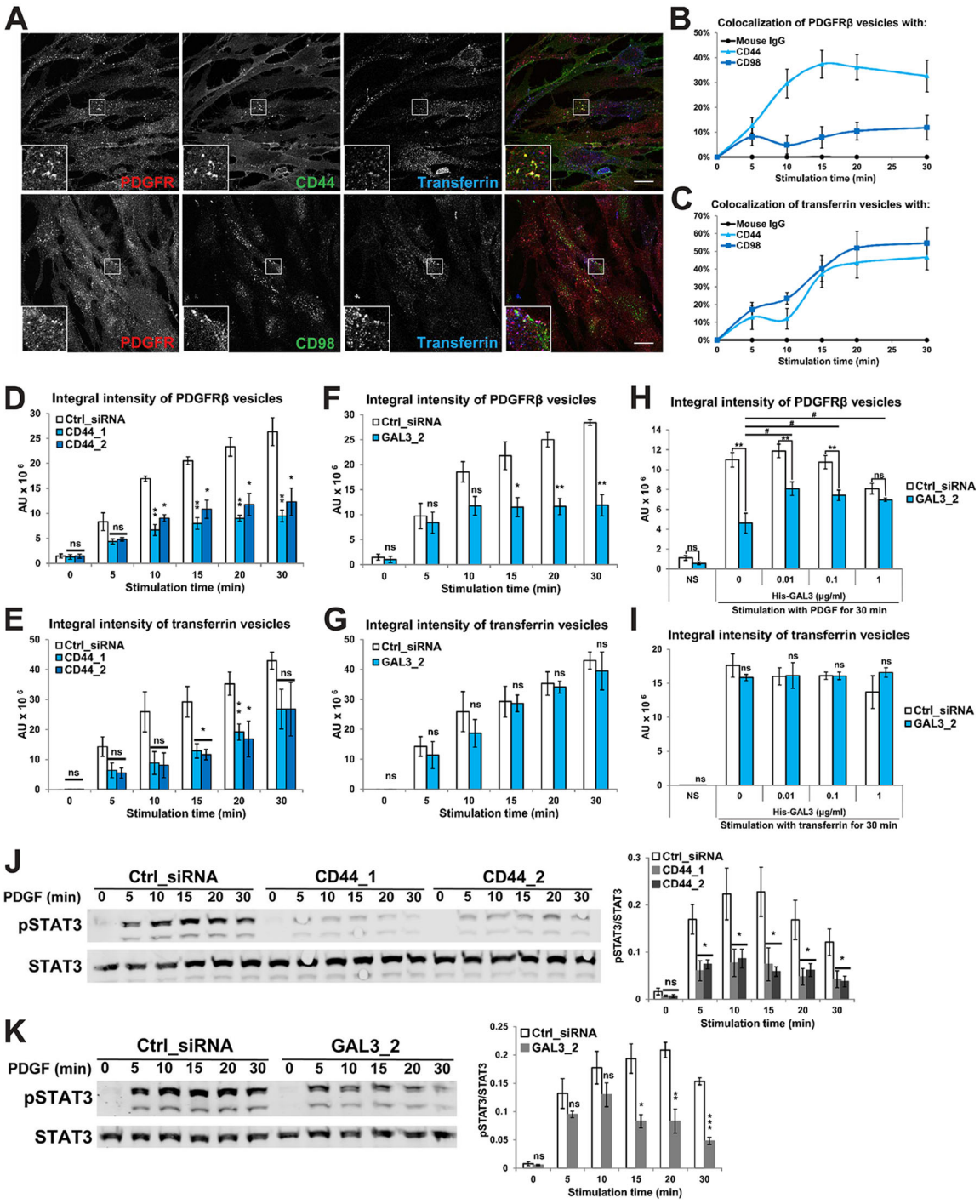

Fig. 4. CD44 and galectin-3 participate in PDGFRβ internalization and PDGF-dependent signaling. (A–C) PDGFRβ colocalizes with CD44. (A) Immunofluorescence analysis for transferrin (blue), PDGFRβ (red), CD44 or CD98 (green) was performed upon stimulation with PDGF-BB, and antibodies against CD44 or CD98 for 10 min. Scale bars: 20 µm. Colocalization of PDGFRβ- (B) or transferrin-positive vesicles (C) with CD44 (light blue), CD98 (dark blue) or control mouse IgG (black) was quantified. Representative of three independent experiments. Results are mean±s.d. of the percentage colocalization calculated from ten randomly selected fields. (D–G) CD44 and galectin-3 are required for PDGFRβ internalization. Immunofluorescence analysis was performed upon silencing of CD44 with two siRNAs (10 nM, numbered _1 or _2; D,E) or galectin-3 (GAL3) with 10 nM siRNA_2 (F,G) or in control siRNA-transfected cells (Ctrl_siRNA) and stimulation with PDGF-BB and transferrin. The integral fluorescence intensities of PDGFRβ- (D,F) or transferrin-positive vesicles (E,G) were quantified. (H,I) Rescue of galectin-3-depleted cells by extracellular addition of recombinant His-tagged galectin-3 (His–GAL3). Cells with galectin-3 knockdown (with 10 nM siRNA GAL3_2) were either left untreated (NS) or stimulated by PDGF-BB and transferrin for 30 min without or with His-GAL3 in the indicated concentrations. The integral fluorescence intensities of PDGFRβ- (H) or transferrin-positive vesicles (I) were quantified. (J,K) PDGF-induced STAT3 phosphorylation depends on CD44 and galectin-3. STAT3 phosphorylation and total abundance were detected by western blotting in lysates of cells depleted of CD44 (J) or galectin-3 (K) or transfected with control siRNA (as in D–G), and stimulated with PDGF-BB. Band intensities were measured and phosphorylated STAT3 (pSTAT3) abundance normalized to total STAT3 abundance (J,K, graphs). Data represent mean±s.e.m. of three (D–G,I,K), four (H) or five (J) independent experiments. ns, not significant; *$P\leq0.05$, **$P\leq0.01$, ***$P\leq0.001$ versus respective control time points; $^{\#}P\leq0.05$ when comparing effects of different galectin-3 concentrations [one-way ANOVA and Dunnett's test (D,E,H,I,J) or Student's *t*-test (F–H,K)].

Journal of Cell Science

Journal of Cell Science (2017) 130, 577-589 doi:10.1242/jcs.191213

GAL3_2 (Fig. S4G). However, under these conditions, uptake of transferrin was also affected at 30 min after ligand addition (Fig. S4H; Table S5). Cumulatively, the involvement of CD44 and galectin-3 indicates that PDGFRβ endocytosis can take place via the CLIC and GPI-enriched early endosomal compartment (GEEC) pathway.

As galectin-3 was described to have both extra- and intra-cellular functions (Haudek et al., 2010; Elola et al., 2015) we verified whether addition of soluble recombinant galectin-3 to galectin-3-depleted cells could rescue the observed defect in PDGFRβ endocytosis. As shown in Fig. 4H, addition of 0.01 or 0.1 µg/ml of His-tagged full-length galectin-3 was able to partially rescue the PDGFRβ internalization that was reduced by galectin-3 knockdown. Consistent with previous observations (Lakshminarayan et al., 2014), a higher (non-physiological) dose of 1 µg/ml galectin-3 inhibited PDGFRβ endocytosis even in control cells (Fig. 4H). Importantly, addition of recombinant galectin-3 did not affect transferrin internalization in control or galectin-3-depleted cells (Fig. 4I). These data indicate that the function of galectin-3 in PDGFRβ endocytosis depends at least in part on its extracellular activity, which mediates receptor clustering as a prerequisite for formation of an endocytic carrier (Johannes et al., 2015). Eventually, we assessed whether inhibition of PDGFRβ uptake mediated by CD44 and galectin-3 had a similar effect on PDGFRβ signaling as depletion of other endocytosis regulators. Indeed, knockdown of CD44 or galectin-3 reduced activation of STAT3 but not other signaling effectors (Fig. 4J,K; Fig. S4I,J).

Different endocytic routes mediate PDGFRβ internalization and PDGF-induced STAT3 activation

Having established that multiple routes can mediate uptake of ligand-stimulated PDGFRβ, we next tested how simultaneous knockdown of different CME and CIE components affected endocytosis of PDGFRβ. To this end, we performed co-depletion of DNM2 with CHC (Fig. 5A,B), ROCK2 (Fig. 5C,D) or galectin-3 (Fig. 5E,F), and measured internalization of PDGFRβ and transferrin (Tables S6–S8). As expected for transferrin internalized primarily via CME, co-silencing of DNM2 with other endocytic components did not inhibit transferrin uptake more than depletion of DNM2 alone (Fig. 5B,D,F). In contrast, at 30 min of PDGF-BB stimulation, we observed an additive effect of co-silencing of DNM2 and CHC on PDGFRβ uptake, when compared to single knockdowns of these proteins (Fig. 5A). This could indicate that co-depletion of DNM2 and CHC reduced PDGFRβ internalization by impairing both CME and dynamin-dependent CIE, consistent with our above results. However, we cannot formally exclude that a stronger decrease in PDGFRβ internalization may be due to a more efficient inhibition of CME upon co-silencing of DNM2 and CHC than the one caused by single knockdowns. In turn, co-depletion of DNM2 with ROCK2 or with galectin-3 showed no additive effects in inhibiting PDGFRβ uptake (Fig. 5C,E). In general, these data suggest existence of compensatory mechanisms, enabling internalization of the receptor at substantial levels even upon impairment of two potential uptake routes.

We then investigated how double silencing of DNM2 with other endocytic components affected PDGF-induced signaling. In accordance with the results on PDGFRβ uptake (Fig. 5A), we observed an additive effect of DNM2 and CHC co-depletion which decreased STAT3 activation more than any of the single knockdowns (Fig. 5G). Combination of DNM2 and ROCK2 depletion did not further alter STAT3 phosphorylation (Fig. 5H), which matches the data on PDGFRβ endocytosis (Fig. 5C). However, co-silencing of DNM2 and galectin-3 led to a stronger impairment of STAT3 activation than depletion of single proteins (Fig. 5I), which is in contrast to the microscopy data showing no additive effects in decreasing PDGFRβ uptake (Fig. 5E). These results may suggest an additional, positive role of galectin-3 in modulating STAT3 activation in response to PDGF-BB, independent of its function in regulating the rate of PDGFRβ endocytosis.

PDGF-induced gene expression is affected by inhibitors of PDGFRβ internalization

Our data suggested that PDGF-induced STAT3 activation required complete internalization of the receptor, independently of a specific uptake route. STAT3 acts as a transcription factor, regulating expression of several PDGF uptake genes, with *MYC* being one of key mediators of a mitogenic response (Bowman et al., 2001; Jones and Kazlauskas, 2001). We previously showed that inhibition of dynamin activity reduced *MYC* expression, downstream of STAT3 activated by PDGF-BB (Sadowski et al., 2013). We now investigated whether inhibition of ROCK1/2 or Cdc42 activity, required for CIE of PDGFRβ, affected expression of *MYC* and other PDGF target genes. To avoid prolonged exposure of cells to pharmacological inhibitors and thus to reduce their unspecific effects, cells were stimulated by pulses of PDGF-BB in the presence of a particular inhibitor, instead of continuous treatment with the ligand. Short pulses of PDGF-BB (30–60 min) have been reported to induce DNA synthesis as efficiently as continuous presence of the ligand for 8 h (Jones and Kazlauskas, 2001), and we applied such a pulse-stimulation regime in our previous study (Sadowski et al., 2013). We first selected a set of 11 known (Bowman et al., 2001; Vij et al., 2008) or predicted (using MotifMap; Daily et al., 2011) STAT3 target genes of which expression was induced upon pulse-stimulation with PDGF-BB, at different chase time points (60–240 min). The expression profiles of these genes upon PDGF pulse induction varied considerably, being early or late, and transient or persistent (Fig. 6A–I; Fig. S4K,L). We then measured whether expression of these genes changed upon pulse stimulation with PDGF-BB in the presence of dynasore, Y-27632 or ML141 (inhibiting dynamin, ROCK1/2 or Cdc42, respectively). We observed different patterns of alterations in 9 of 11 genes, while expression of *RELB* and *JUNB* was not affected by any inhibitor (Fig. S4K,L). Expression of *MYC* and *IL8*, which are the best established and experimentally verified targets of PDGF-induced STAT3 activity, were equally reduced by all three inhibitors (Fig. 6A,B). Similar effects were observed for *EGR1* and *EGR3* (Fig. 6D,F). Expression of *EGR2* and *FOSL1* was preferentially inhibited by dynasore (Fig. 6E,H), while expression of *HBEGF* was preferentially inhibited by Y-27632 (Fig. 6C). However, in some cases, the impact of inhibitors varied depending on the time point of measurement (e.g. *EGR2* in Fig. 6E; *FOSB* in Fig. 6G; *ATF3* in Fig. 6I). This suggests that the expression pattern of a given target gene may be differently sensitive to a particular inhibition in the course of time, likely due to several other transcription factors binding to their promoters beside STAT3.

PDGF-induced DNA synthesis is impaired by inhibitors of CIE

We previously showed that inhibition of dynamin activity, which impaired PDGFRβ endocytosis and STAT3 activation, caused weaker induction of DNA synthesis, as a part of mitogenic response to PDGF-BB (Sadowski et al., 2013). We now verified whether interference with activity of regulators of CIE affected the mitogenic response to PDGF-BB. When we treated serum-starved cells with PDGF-BB for 1 h in the presence of a solvent control, the percentage of cells undergoing DNA synthesis (measured by BrdU incorporation after 24 h) was increased by about threefold

Journal of Cell Science (2017) 130, 577-589 doi:10.1242/jcs.191213

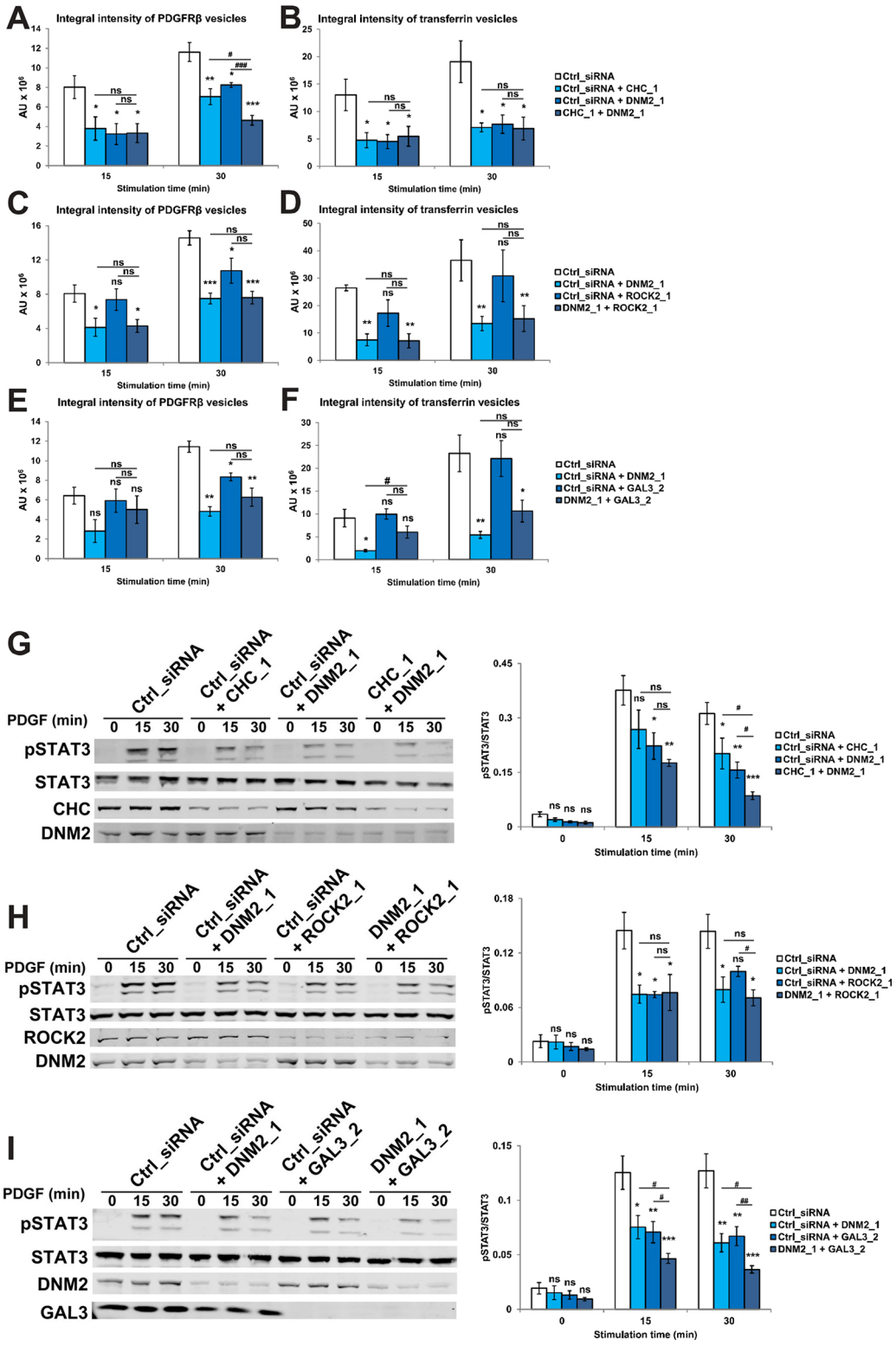

Fig. 5. Different endocytic routes mediate PDGFRβ internalization and PDGF-induced STAT3 activation. (A–I) Effects of co-depletion of DNM2 and other endocytic components on PDGFRβ uptake (A,C,E), transferrin internalization (B,D,F) and STAT3 activation (G–I). Cells were transfected with siRNAs against DNM2 (30 nM; A–I), CHC (30 nM; A,B,G), ROCK2 (10 nM; C,D,H) or GAL3 (10 nM; E,F,I) plus control siRNA (Ctrl_siRNA; 10 nM in C–F and H–I, or 30 nM in A,B, G) to equalize amount of siRNA used. Control cells were transfected with Ctrl_siRNA alone (60 nM in A, B, G or 40 nM in C–F,H–I). Cells were stimulated with PDGF-BB (A–I) and transferrin (A–F) for the indicated times. (A–F) Immunofluorescence analysis was performed to measure the integral fluorescence intensities of PDGFRβ- (A,C,E) or transferrin-positive vesicles (B,D,F). (G–I) Alternatively, following lysis, STAT3 phosphorylation and total abundance were detected by western blotting. Band intensities were measured and phosphorylated STAT3 (pSTAT3) abundance was normalized to total STAT3 abundance (G–I, graphs). Data represent mean±s.e.m. of four (A–H) or six (I) independent experiments. ns, not significant; $^{*}P\leq0.05$, $^{**}P\leq0.01$, $^{***}P\leq0.001$ when compared to control siRNA (one-way ANOVA and Dunnett's test); ns, not significant; $^{\#}P\leq0.05$, $^{\#\#}P\leq0.01$, $^{\#\#\#}P\leq0.001$, when comparing a selected single knockdown to a double knockdown (Student's *t*-test).

Journal of Cell Science

Journal of Cell Science (2017) 130, 577-589 doi:10.1242/jcs.191213

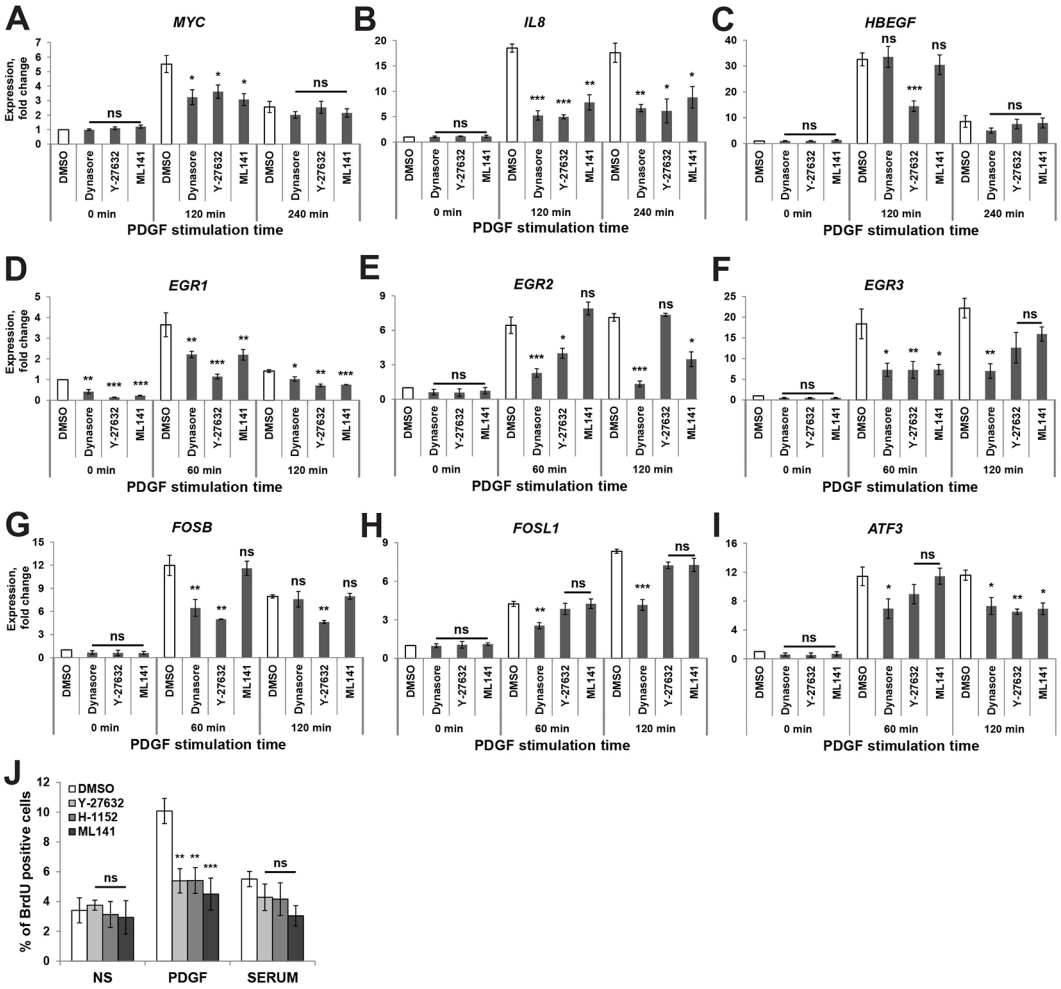

Fig. 6. Activities of dynamin, ROCK1/2 and Cdc42 contribute to PDGF-induced transcriptional and mitogenic response. (A–I) PDGF-induced gene expression requires functional dynamin, ROCK1/2 and Cdc42. Expression of nine PDGF-BB target genes (indicated above graphs) was measured by qRT-PCR upon treatment with inhibitors of dynamin (dynasore), ROCK1/2 (Y-27632), Cdc42 (ML141) or DMSO and stimulation with PDGF-BB. (J) PDGF-induced mitogenic response is impaired upon inhibition of ROCK1/2 or Cdc42. DNA synthesis was measured by BrdU incorporation in cells treated with inhibitors of ROCK1/2 (Y-27632, H-1152) or Cdc42 (ML141), or with DMSO and stimulated with PDGF-BB (1 h), 10% serum or left unstimulated (NS). Data represent mean±s.e.m. of five (A,C and J), three (B,D–H) or four (I) independent experiments. ns, not significant; *$P\leq0.05$, **$P\leq0.01$, ***$P\leq0.001$ versus control (one-way ANOVA and Dunnett's test).

(Fig. 6J). Under similar conditions, stimulation of cells with 10% serum for 1 h caused an insignificant, less than twofold, induction of DNA synthesis. When the pulse of PDGF-BB was administered in the presence of ROCK inhibitors Y-27632 and H-1152 or in the presence of Cdc42 inhibitor ML141, induction of DNA synthesis was reduced by ∼50% (Fig. 6J). These data suggest that inhibition of ROCK1/2 and Cdc42, which impairs PDGFRβ internalization by CIE and STAT3 activation, correlate with diminished PDGF-induced mitogenic response.

DISCUSSION

In this study, we report that ligand-induced internalization of PDGFRβ can occur via multiple endocytic pathways, and we characterize their selected molecular determinants. We demonstrate that in human fibroblasts expressing endogenous PDGFRβ and stimulated with 50 ng/ml PDGF-BB, uptake of this receptor proceeds via parallel routes of CME and CIE. In turn, CME represents a predominant uptake route of PDGFRβ when cells are stimulated with lower doses of the ligand (10 ng/ml), similar to as reported for EGFR (Sigismund et al., 2005, 2008). CME of PDGFRβ involves the canonical AP2 complex as a clathrin adaptor and dynamin as a scission-mediating molecule. Inactivation of AP2-dependent CME in cells treated with 50 ng/ml PDGF-BB decreased uptake of PDGFRβ by ∼50%, suggesting that residual entry of the receptor proceeded via CIE. Thus, our data clearly demonstrate existence of clathrin-independent entry routes for PDGFRβ which, however, cannot provide a full compensation for the lack of CME.

Through dissection of the molecular machinery of CIE mediating PDGFRβ uptake, we confirmed the requirement for actin cytoskeleton and the selective involvement of RhoA and Cdc42 but not Rac1. The participation of RhoA and Cdc42 suggests that CIE of PDGFRβ may proceed via more than one mechanism. The activity of Cdc42 is known to be required for the CLIC and GEEC route (Lundmark et al., 2008; Francis et al., 2015). This pathway mediates uptake of CD44 as a typical cargo molecule and involves galectin-3 as an extracellular clustering adaptor that drives the formation of endocytic intermediates (Lakshminarayan et al., 2014). We found both CD44 and galectin-3 to be involved in uptake of PDGFRβ. Interestingly, the impairment of endocytosis of PDGFRβ upon depletion of galectin-3 could be partially rescued by addition of recombinant galectin-3, suggesting that the extracellular pool of this protein participates in clustering and uptake of PDGFRβ by CIE

Journal of Cell Science (2017) 130, 577-589 doi:10.1242/jcs.191213

(Johannes et al., 2015). In case of CD44, its interaction with PDGFRβ was previously described to regulate receptor signaling (Li et al., 2006; Misra et al., 2006; Porsch et al., 2014). Interestingly, PDGFRβ was identified as an interacting partner of galectin-3, similarly to CD44 (Lakshminarayan et al., 2014). Therefore, the associations between galectin-3, CD44 and PDGFRβ could mediate incorporation of the receptor into the forming CLIC structures for subsequent uptake. Overall, the involvement of Cdc42, galectin-3 and CD44 strongly argues that the CLIC and GEEC pathway contributes to PDGFRβ internalization.

The function of RhoA and its downstream effectors ROCK1/2 in endocytosis of PDGFRβ is more difficult to interpret. RhoA was reported to act in fast endophilin-mediated endocytosis (FEME), a recently characterized CIE pathway that mediates uptake of ligand-induced GPCRs and RTKs, including PDGFR (Boucrot et al., 2015; Renard et al., 2015). However, FEME was described to depend also on the activity of Rac1, and we did not observe the effect of Rac1 inhibition on PDGFRβ internalization in our study, possibly due to cell type-specific differences. Based on our data and the published results (Boucrot et al., 2015), it is nevertheless likely that FEME is involved in uptake of PDGFRβ, as another CIE mechanism operating in parallel to the CLIC and GEEC pathway. While FEME requires the activity of dynamin for scission of endocytic intermediates, the CLIC and GEEC pathway is independent of it. The impaired internalization of PDGFRβ that we observed upon dynamin depletion or inhibition of its activity (Sadowski et al., 2013 and this study) could result from the involvement of dynamin in both CME and FEME of the receptor.

Based on our data, we cannot estimate the exact proportions of PDGFRβ that is internalized via different uptake routes under unperturbed conditions. We observed that interfering with the components of CME, Cdc42 or RhoA–ROCK caused in each case a substantial reduction in PDGFRβ internalization. On the one side, this indicates that when one uptake mechanism is dysfunctional, the other(s) cannot fully compensate for it, otherwise impairment in PDGFRβ endocytosis would not be observed. On the other side, partial functional compensation must operate between individual uptake pathways, as indicated by our data on co-depletion of CME and CIE components. We expected that such attempts should strongly and additively inhibit internalization of PDGFRβ. However, we could only achieve this to a moderate degree by simultaneous knockdown of DNM2 along with CHC, but not with ROCK2 or galectin-3. It was reported that only very efficient depletion of CHC or DNM2 caused strong inhibition of EGFR uptake, while transferrin endocytosis was impaired even upon less efficient knockdown (Huang et al., 2004). It is therefore possible that in our hands the extent of protein depletion was insufficient (particularly in case of technically difficult double knockdowns) to observe stronger inhibition of PDGFRβ endocytosis. We nevertheless favor the view that the homeostatic mechanisms of the cell act to rescue defects in one uptake mechanism by increased cargo flow along other routes. Such global co-regulation of cellular entry pathways may be facilitated by some shared components. The actin cytoskeleton could represent one of them, as beside CIE it also contributes to CME, depending on the cell type and cargo (Lamaze et al., 1997; Ferguson et al., 2009; Mooren et al., 2012). Still, our data argue that the entry routes of PDGFRβ are not fully interchangeable. By comparison, internalization of EGFR upon stimulation with 100 ng/ml EGF was reported to occur with ∼60% via CME and ∼40% via CIE (Sigismund et al., 2008). While it is unclear which mechanisms sort the receptor towards CME or CIE, it is possible that certain regions of the cell may favor particular routes, e.g. FEME and CLIC were postulated to occur preferentially at the leading edges of migrating cells (Howes et al., 2010; Boucrot et al., 2015).

With respect to PDGFRβ signaling, we found no evidence for a particular internalization mechanism being linked to the activation of one specific pathway or to transcriptional induction of a specific set of PDGF target genes. A number of signaling effectors of PDGFRβ, such as AKT proteins, PLCγ or GSK3β, were not affected by inhibiting CME or CIE. Interestingly, activation of STAT3 was prominently impaired by interfering with any endocytic components that reduced PDGFRβ internalization. This clearly indicates that PDGFRβ endocytosis, independently of the exact uptake route, is required for full activation of STAT3. This is consistent with the notion that sustained STAT3 activation occurs in part from endosomes, after PDGFRβ internalization. The presence of phosphorylated STAT3 on endosomes was previously reported in cells stimulated with other growth factors (EGF, hepatocyte growth factor) or cytokines (interleukin-6) (Bild et al., 2002; Kermorgant and Parker, 2008; German et al., 2011). Our data suggest that the overall amount of (likely phosphorylated) PDGFRβ on endosomes specifies the level of STAT3 activation and the subsequent mitogenic response to PDGF-BB. In case of internalized EGFR, it was shown that cells maintain a constant mean amount of phosphorylated EGFR per endosome, which is important for determining the amplitude and duration of signaling, and for subsequent cell fate specification (Villaseñor et al., 2015). In our system, full STAT3 activation could also be viewed as a detector of the integrity of the endocytic pathway. Defects in any of the internalization mechanisms, reducing the levels of phosphorylated STAT3, would be restrictive for cell cycle progression. Cumulatively, our results reinforce the notion that internalization and endosomal compartmentalization regulate the signaling of the activated growth factor receptors in space and time.

MATERIALS AND METHODS

Antibodies and chemicals

Primary antibodies are listed in Table S9. Secondary antibodies and transferrin–Alexa-Fluor-647 used for immunofluorescence were from Invitrogen. Secondary donkey antibodies for western blotting infrared-based detection were from LI-COR Biotechnology. Dynasore (324410), H-1152 (555550), NSC23766 (553502), Rhosin (S1555460) were from Merck; latrunculin A (L5163), ML141 (SML0407) and Y-27632 (Y0503) were from Sigma-Aldrich. Inhibitors were used at the following concentrations: dynasore, 80 µM; H-1152, 10 µM; latrunculin A, 5 ng/ml; ML141, 10 µM; NSC23766, 50 µM; Rhosin, 30 µM; and Y-27632, 10 µM. The recombinant full-length His-tagged galectin-3 was a kind gift from Ludger Johannes, Institute Curie, Paris. The C3 toxin was expressed and purified as described previously (Sahai and Olson, 2006) with the following adjustments: bacteria were lysed with ice-cold lysis buffer A (50 mM Tris-HCl pH 7.5, 5 mM $MgCl_2$, 50 mM NaCl, 1 mM DTT, 2 mM PMSF) instead of TBS buffer. Samples were kept on ice while being disrupted by six 10 s blasts of sonication using MiSonix Sonicator 3000, followed by removal of debris by centrifugation at 10,000 ***g*** for 20 min at 4°C. Ice-cold buffer A was used for subsequent washes instead of TBS buffer. C3 toxin was used at the concentration of 5 µg/ml. DMSO (BioShop Canada) served in an equivalent volume as control for all inhibitors. PDGF-BB was from PeproTech (#100-14B).

Plasmids

pGEX-KG TAT-Myc-C3 toxin and pcDNA-GFP vectors (i.e. pcDNA vector expressing Rac1 WT, Rac1-T17N, Rac1-Q61L, RhoA WT, RhoA-Q63L, RhoA-T19N, Cdc42 WT, Cdc42-T17N and Cdc42-Q61L tagged with GFP) were a kind gift from Neil Hotchin (University of Birmingham, School of Biosciences, UK).

Small interfering RNA

Ambion Silencer Select siRNAs were from ThermoFisher Scientific and ON-TARGETplus siRNA were from GE Dharmacon. See Table S10 for

Journal of Cell Science (2017) 130, 577-589 doi:10.1242/jcs.191213

full details. As negative control, non-specific Silencer Select siRNA oligonucleotide (4390843) was used.

Cell transfection

Transfections were performed according to manufacturers' instructions using jetPEI (Polyplus Transfection) for DNA and Lipofectamine RNAiMAX (Life Technologies) or INTERFERin (Polyplus Transfection) for siRNA, and analyzed 24 h after DNA or 72 h after siRNA transfection.

Cell culture and treatments

CCD-1070Sk human normal foreskin fibroblasts were purchased from ATCC (CRL-2091) and maintained in MEM supplemented with 10% fetal bovine serum (FBS), 2 mM L-glutamine (all from Sigma-Aldrich), in 5% CO_2 at 37°C. Cells were routinely tested for mycoplasma contamination.

Cells were plated either directly in 12-well plates (1×10^5/well) for western blotting, in 6-well dishes (2×10^5/well) for quantitative real-time PCR (qRT-PCR), 96-well plates (1×10^4/well) for BrdU incorporation, or seeded on 12-mm coverslips in 24-well plates (5×10^4/well) for immunofluorescence analysis. One day after plating, cells were serum-starved overnight before every treatment. Alternatively, cells were serum-starved in the presence of C3 toxin or Rhosin 16 h prior to PDGF-BB stimulation.

Unless indicated otherwise, stimulation was performed with 50 ng/ml PDGF-BB, for immunofluorescence experiments in combination with 25 µg/ml transferrin–Alexa-Fluor-647, for the indicated time periods with or without inhibitors or recombinant galectin-3. Directly before stimulation cells were transferred to CO_2-independent medium in a non-CO_2 37°C incubator. Dynasore, H-1152, ML141, NSC23766, Y-27632 were applied to cells 30 min before and during PDGF-BB stimulation, whereas latrunculin A was only added 5 min before stimulation. Recombinant galectin-3 was added with PDGF-BB and transferrin at 0.01-1 µg/ml.

Western blot analysis

Western blotting analysis was as described previously (Sadowski et al., 2013).

Immunofluorescence staining and image analysis

Following stimulation, cells were transferred to ice, washed twice with ice-cold PBS, and ice-cold 3.6% paraformaldehyde was added for 15 min. Cells were washed three times with PBS and processed directly for immunofluorescence as described previously (Sadowski et al., 2013). Slides were scanned using a LSM 710 confocal microscope (Zeiss) with EC-Plan-Neofluar 40×1.3 NA oil immersion objective. ZEN 2009 software (Zeiss) was used for acquisition. At least ten 12-bit images with resolution 1024×1024 pixels were acquired per experimental condition. Images were imported into MotionTracking (http://motiontracking.mpi-cbg.de) to analyze integral fluorescence of a particular marker in all vesicles (expressed in arbitrary units, AU) and the percentage of colocalization between two markers (Rink et al., 2005; Collinet et al., 2010; Kalaidzidis et al., 2015). Pictures were assembled in Photoshop (Adobe) with only linear adjustments of contrast and brightness.

CD44 and CD98 internalization assay

Cells were plated as for immunofluorescence analysis and treated with 10 µg/ml antibodies against CD44, CD98 or with mouse IgG (I8765, Sigma-Aldrich), along with PDGF-BB and transferrin for the indicated time periods at 37°C. Internalization was terminated by transferring cells to ice. To remove surface-bound antibodies, cells were washed with 0.5% acetic acid in 0.5 M NaCl for 30 s and three times with ice-cold PBS, and processed for immunofluorescence staining.

qRT-PCR

Cells, plated as described above, were treated with a 30 or 60 min pulse of PDGF-BB with or without the indicated inhibitors. Control cells were left unstimulated (no PDGF), but treated with inhibitors for 30 min. Cells were either lysed or (after a 60 min pulse) washed twice with PBS, serum-starved for 60 or 180 min and then lysed. Total RNA was isolated from cell lysates by using a GenElute Mammalian Total RNA Miniprep kit and cleaned by using a DNase I Amplification Grade according to the manufacturer's protocols (Sigma-Aldrich). cDNA was synthesized using M-MLV reverse transcriptase (Sigma-Aldrich). Primers (Table S11) were designed using QuantPrime software (http://www.quantprime.de/) (Arvidsson et al., 2008). qRT-PCR was performed with a Kapa SYBR FAST qPCR kit (Kapa Biosystems) according to the manufacturer's protocol using a 7900HT fast real-time PCR system (Applied Biosystems). Data were quantified using RQ Manager v1.21 and Data Assist v2.0 software (Applied Biosystems) and normalized to the level of *ACTB* (actin) and *B2M* (β2-microglobulin) mRNAs. The relative quantification method was used to estimate the fold change of gene expression.

Bromodeoxyuridine incorporation

Cell proliferation was tested by bromodeoxyuridine (BrdU) incorporation. Cells were seeded in 96-well plates (Greiner) (10^4 cells/well) and treated as described above with PDGF-BB, or 10% serum, or left non-stimulated with or without the indicated inhibitors for 1 h. After two washes with PBS, cells were transferred to serum-free medium with 10 µM BrdU for 23 h. Then, cells were fixed and processed as described previously (Sadowski et al., 2013). Cells were viewed with Olympus Scan^R/Cell^R with UPLSAPO 40×0.95 NA objective. For each condition, two-channel images (BrdU and DAPI) of 50–60 randomly selected fields were acquired. Images were analyzed with Olympus Scan^R software.

Statistical analysis

At least three independent experiments were performed in each case. Statistical testing was performed using Prism 6 (GraphPad Software). Data were analyzed for Gaussian distribution with a Kolmogorov–Smirnov test with the Dallal–Wilkinson–Lillie test for corrected *P* value. In case of Gaussian distribution, the following parametric tests were used: Student's *t*-test (two groups) or one-way ANOVA and Dunnett's test (>2 groups), as appropriate. In case of non-Gaussian distribution, the following non-parametric tests were used: two-tailed Mann–Whitney U-test (two groups) or Kruskal–Wallis one-way ANOVA and Dunnett's test (>2 groups), as appropriate. Significance of mean comparison is annotated as follows: ns, non-significant ($P>0.05$), *$P\leq0.05$, **$P\leq0.01$ and ***$P\leq0.001$. No statistical methods were used to predetermine sample size.

Acknowledgements

We are grateful to Dr Ludger Johannes for his gift of recombinant galectin-3. We thank Dr Neil Hotchin for providing plasmids. We acknowledge Dr Jarosław Cendrowski, Marta Kaczmarek and Agata Poświata for critical reading of the manuscript.

Competing interests

The authors declare no competing or financial interests.

Author contributions

K.J. conceived, designed, performed and analyzed experiments and wrote the manuscript; D.Z.-B. and A.M. performed experiments; Y.K. and C.H. helped in conceiving and/or analyzing the experiments and provided reagents; M.M. conceived, designed and analyzed experiments and wrote the manuscript.

Funding

This work was supported by a grant from Fundacja na rzecz Nauki Polskiej (Foundation for Polish Science) within the International PhD Project 'Studies of nucleic acids and proteins-from basic to applied research', co-financed from the European Regional Development Fund, and by a Narodowe Centrum Nauki (National Science Center) MAESTRO grant (UMO-2011/02/A/NZ3/00149) to M.M.

Supplementary information

Supplementary information available online at
http://jcs.biologists.org/lookup/doi/10.1242/jcs.191213.supplemental

References

Akbar, H., Cancelas, J., Williams, D. A., Zheng, J. and Zheng, Y. (2006). Rational design and applications of a Rac GTPase-specific small molecule inhibitor. *Methods Enzymol.* **406**, 554-565.

Andrae, J., Gallini, R. and Betsholtz, C. (2008). Role of platelet-derived growth factors in physiology and medicine. *Genes Dev.* **22**, 1276-1312.

Arvidsson, S., Kwasniewski, M., Riano-Pachon, D. M. and Mueller-Roeber, B. (2008). QuantPrime–a flexible tool for reliable high-throughput primer design for quantitative PCR. *BMC Bioinformatics* **9**, 465.

Bild, A. H., Turkson, J. and Jove, R. (2002). Cytoplasmic transport of Stat3 by receptor-mediated endocytosis. *EMBO J.* **21**, 3255-3263.
Boucrot, E., Ferreira, A. P., Almeida-Souza, L., Debard, S., Vallis, Y., Howard, G., Bertot, L., Sauvonnet, N. and McMahon, H. T. (2015). Endophilin marks and controls a clathrin-independent endocytic pathway. *Nature* **517**, 460-465.
Bowman, T., Broome, M. A., Sinibaldi, D., Wharton, W., Pledger, W. J., Sedivy, J. M., Irby, R., Yeatman, T., Courtneidge, S. A. and Jove, R. (2001). Stat3-mediated Myc expression is required for Src transformation and PDGF-induced mitogenesis. *Proc. Natl. Acad. Sci. USA* **98**, 7319-7324.
Collinet, C., Stoter, M., Bradshaw, C. R., Samusik, N., Rink, J. C., Kenski, D., Habermann, B., Buchholz, F., Henschel, R., Mueller, M. S. et al. (2010). Systems survey of endocytosis by multiparametric image analysis. *Nature* **464**, 243-249.
Daily, K., Patel, V. R., Rigor, P., Xie, X. and Baldi, P. (2011). MotifMap: integrative genome-wide maps of regulatory motif sites for model species. *BMC Bioinformatics* **12**, 495.
De Donatis, A., Comito, G., Buricchi, F., Vinci, M. C., Parenti, A., Caselli, A., Camici, G., Manao, G., Ramponi, G. and Cirri, P. (2008). Proliferation versus migration in platelet-derived growth factor signaling: the key role of endocytosis. *J. Biol. Chem.* **283**, 19948-19956.
Doherty, G. J. and McMahon, H. T. (2009). Mechanisms of endocytosis. *Annu. Rev. Biochem.* **78**, 857-902.
Elola, M. T., Blidner, A. G., Ferragut, F., Bracalente, C. and Rabinovich, G. A. (2015). Assembly, organization and regulation of cell-surface receptors by lectin-glycan complexes. *Biochem. J.* **469**, 1-16.
Eyster, C. A., Higginson, J. D., Huebner, R., Porat-Shliom, N., Weigert, R., Wu, W. W., Shen, R.-F. and Donaldson, J. G. (2009). Discovery of new cargo proteins that enter cells through clathrin-independent endocytosis. *Traffic* **10**, 590-599.
Ferguson, S. M., Raimondi, A., Paradise, S., Shen, H., Mesaki, K., Ferguson, A., Destaing, O., Ko, G., Takasaki, J., Cremona, O. et al. (2009). Coordinated actions of actin and BAR proteins upstream of dynamin at endocytic clathrin-coated pits. *Dev. Cell* **17**, 811-822.
Francis, M. K., Holst, M. R., Vidal-Quadras, M., Henriksson, S., Santarella-Mellwig, R., Sandblad, L. and Lundmark, R. (2015). Endocytic membrane turnover at the leading edge is driven by a transient interaction between Cdc42 and GRAF1. *J. Cell Sci.* **128**, 4183-4195.
German, C. L., Sauer, B. M. and Howe, C. L. (2011). The STAT3 beacon: IL-6 recurrently activates STAT 3 from endosomal structures. *Exp. Cell Res.* **317**, 1955-1969.
Goh, L. K. and Sorkin, A. (2013). Endocytosis of receptor tyrosine kinases. *Cold Spring Harb. Perspect. Biol.* **5**, a017459.
Gonnord, P., Blouin, C. M. and Lamaze, C. (2012). Membrane trafficking and signaling: two sides of the same coin. *Semin. Cell Dev. Biol.* **23**, 154-164.
Grassart, A., Dujeancourt, A., Lazarow, P. B., Dautry-Varsat, A. and Sauvonnet, N. (2008). Clathrin-independent endocytosis used by the IL-2 receptor is regulated by Rac1, Pak1 and Pak2. *EMBO Rep.* **9**, 356-362.
Haudek, K. C., Spronk, K. J., Voss, P. G., Patterson, R. J., Wang, J. L. and Arnoys, E. J. (2010). Dynamics of galectin-3 in the nucleus and cytoplasm. *Biochim. Biophys. Acta* **1800**, 181-189.
Heldin, C. H. and Westermark, B. (1999). Mechanism of action and in vivo role of platelet-derived growth factor. *Physiol. Rev.* **79**, 1283-1316.
Howes, M. T., Kirkham, M., Riches, J., Cortese, K., Walser, P. J., Simpson, F., Hill, M. M., Jones, A., Lundmark, R., Lindsay, M. R. et al. (2010). Clathrin-independent carriers form a high capacity endocytic sorting system at the leading edge of migrating cells. *J. Cell Biol.* **190**, 675-691.
Huang, F., Khvorova, A., Marshall, W. and Sorkin, A. (2004). Analysis of clathrin-mediated endocytosis of epidermal growth factor receptor by RNA interference. *J. Biol. Chem.* **279**, 16657-16661.
Irannejad, R., Tsvetanova, N. G., Lobingier, B. T. and Von Zastrow, M. (2015). Effects of endocytosis on receptor-mediated signaling. *Curr. Opin. Cell Biol.* **35**, 137-143.
Johannes, L., Parton, R. G., Bassereau, P. and Mayor, S. (2015). Building endocytic pits without clathrin. *Nat. Rev. Mol. Cell Biol.* **16**, 311-321.
Jones, S. M. and Kazlauskas, A. (2001). Growth-factor-dependent mitogenesis requires two distinct phases of signalling. *Nat. Cell Biol.* **3**, 165-172.
Kalaidzidis, Y., Kalaidzidis, I. and Zerial, M. (2015). A probabilistic method to quantify the colocalization of markers on intracellular vesicular structures visualized by light microscopy. *AIP Conf. Proc.* **1641**, 580-587.
Kapeller, R., Chakrabarti, R., Cantley, L., Fay, F. and Corvera, S. (1993). Internalization of activated platelet-derived growth factor receptor-phosphatidylinositol-3′ kinase complexes: potential interactions with the microtubule cytoskeleton. *Mol. Cell. Biol.* **13**, 6052-6063.
Kermorgant, S. and Parker, P. J. (2008). Receptor trafficking controls weak signal delivery: a strategy used by c-Met for STAT3 nuclear accumulation. *J. Cell Biol.* **182**, 855-863.
Lakshminarayan, R., Wunder, C., Becken, U., Howes, M. T., Benzing, C., Arumugam, S., Sales, S., Ariotti, N., Chambon, V., Lamaze, C. et al. (2014). Galectin-3 drives glycosphingolipid-dependent biogenesis of clathrin-independent carriers. *Nat. Cell Biol.* **16**, 595-606.
Lamaze, C., Fujimoto, L. M., Yin, H. L. and Schmid, S. L. (1997). The actin cytoskeleton is required for receptor-mediated endocytosis in mammalian cells. *J. Biol. Chem.* **272**, 20332-20335.
Lamaze, C., Dujeancourt, A., Baba, T., Lo, C. G., Benmerah, A. and Dautry-Varsat, A. (2001). Interleukin 2 receptors and detergent-resistant membrane domains define a clathrin-independent endocytic pathway. *Mol. Cell* **7**, 661-671.
Li, L., Heldin, C. H. and Heldin, P. (2006). Inhibition of platelet-derived growth factor-BB-induced receptor activation and fibroblast migration by hyaluronan activation of CD44. *J. Biol. Chem.* **281**, 26512-26519.
Lundmark, R., Doherty, G. J., Howes, M. T., Cortese, K., Vallis, Y., Parton, R. G. and McMahon, H. T. (2008). The GTPase-activating protein GRAF1 regulates the CLIC/GEEC endocytic pathway. *Curr. Biol.* **18**, 1802-1808.
Mayor, S., Parton, R. G. and Donaldson, J. G. (2014). Clathrin-independent pathways of endocytosis. *Cold Spring Harb. Perspect. Biol.* **6**, a016758.
McMahon, H. T. and Boucrot, E. (2011). Molecular mechanism and physiological functions of clathrin-mediated endocytosis. *Nat. Rev. Mol. Cell Biol.* **12**, 517-533.
Miaczynska, M. (2013). Effects of membrane trafficking on signaling by receptor tyrosine kinases. *Cold Spring Harb. Perspect. Biol.* **5**, a009035.
Misra, S., Toole, B. P. and Ghatak, S. (2006). Hyaluronan constitutively regulates activation of multiple receptor tyrosine kinases in epithelial and carcinoma cells. *J. Biol. Chem.* **281**, 34936-34941.
Mooren, O. L., Galletta, B. J. and Cooper, J. A. (2012). Roles for actin assembly in endocytosis. *Annu. Rev. Biochem.* **81**, 661-686.
Narumiya, S., Sekine, A. and Fujiwara, M. (1988). Substrate for botulinum ADP-ribosyltransferase, Gb, has an amino acid sequence homologous to a putative rho gene product. *J. Biol. Chem.* **263**, 17255-17257.
Nilsson, J., Thyberg, J., Heldin, C. H., Westermark, B. and Wasteson, A. (1983). Surface binding and internalization of platelet-derived growth factor in human fibroblasts. *Proc. Natl. Acad. Sci. USA* **80**, 5592-5596.
Porsch, H., Mehic, M., Olofsson, B., Heldin, P. and Heldin, C. H. (2014). Platelet-derived growth factor beta-receptor, transforming growth factor beta type I receptor, and CD44 protein modulate each other's signaling and stability. *J. Biol. Chem.* **289**, 19747-19757.
Renard, H.-F., Simunovic, M., Lemière, J., Boucrot, E., Garcia-Castillo, M. D., Arumugam, S., Chambon, V., Lamaze, C., Wunder, C., Kenworthy, A. K. et al. (2015). Endophilin-A2 functions in membrane scission in clathrin-independent endocytosis. *Nature* **517**, 493-496.
Riento, K. and Ridley, A. J. (2003). Rocks: multifunctional kinases in cell behaviour. *Nat. Rev. Mol. Cell Biol.* **4**, 446-456.
Rink, J., Ghigo, E., Kalaidzidis, Y. and Zerial, M. (2005). Rab conversion as a mechanism of progression from early to late endosomes. *Cell* **122**, 735-749.
Sadowski, Ł., Jastrzębski, K., Kalaidzidis, Y., Heldin, C.-H., Hellberg, C. and Miaczynska, M. (2013). Dynamin inhibitors impair endocytosis and mitogenic signaling of PDGF. *Traffic* **14**, 725-736.
Sahai, E. and Olson, M. F. (2006). Purification of TAT-C3 exoenzyme. *Methods Enzymol.* **406**, 128-140.
Shang, X., Marchioni, F., Sipes, N., Evelyn, C. R., Jerabek-Willemsen, M., Duhr, S., Seibel, W., Wortman, M. and Zheng, Y. (2012). Rational design of small molecule inhibitors targeting RhoA subfamily Rho GTPases. *Chem. Biol.* **19**, 699-710.
Sigismund, S., Woelk, T., Puri, C., Maspero, E., Tacchetti, C., Transidico, P., Di Fiore, P. P. and Polo, S. (2005). Clathrin-independent endocytosis of ubiquitinated cargos. *Proc. Natl. Acad. Sci. USA* **102**, 2760-2765.
Sigismund, S., Argenzio, E., Tosoni, D., Cavallaro, E., Polo, S. and Di Fiore, P. P. (2008). Clathrin-mediated internalization is essential for sustained EGFR signaling but dispensable for degradation. *Dev. Cell* **15**, 209-219.
Sigismund, S., Confalonieri, S., Ciliberto, A., Polo, S., Scita, G. and Di Fiore, P. P. (2012). Endocytosis and signaling: cell logistics shape the eukaryotic cell plan. *Physiol. Rev.* **92**, 273-366.
Surviladze, Z., Waller, A., Strouse, J. J., Bologa, C., Ursu, O., Salas, V., Parkinson, J. F., Phillips, G. K., Romero, E., Wandinger-Ness, A. et al. (2010). A Potent and Selective Inhibitor of Cdc42 GTPase. In *Probe Reports from the NIH Molecular Libraries Program*. Bethesda, MD.
Tamura, M., Nakao, H., Yoshizaki, H., Shiratsuchi, M., Shigyo, H., Yamada, H., Ozawa, T., Totsuka, J. and Hidaka, H. (2005). Development of specific Rho-kinase inhibitors and their clinical application. *Biochim. Biophys. Acta* **1754**, 245-252.
Uehata, M., Ishizaki, T., Satoh, H., Ono, T., Kawahara, T., Morishita, T., Tamakawa, H., Yamagami, K., Inui, J., Maekawa, M. et al. (1997). Calcium sensitization of smooth muscle mediated by a Rho-associated protein kinase in hypertension. *Nature* **389**, 990-994.
Vij, N., Sharma, A., Thakkar, M., Sinha, S. and Mohan, R. R. (2008). PDGF-driven proliferation, migration, and IL8 chemokine secretion in human corneal fibroblasts involve JAK2-STAT3 signaling pathway. *Mol. Vis.* **14**, 1020-1027.
Villaseñor, R., Nonaka, H., Del Conte-Zerial, P., Kalaidzidis, Y. and Zerial, M. (2015). Regulation of EGFR signal transduction by analogue-to-digital conversion in endosomes. *Elife* **4**, e06156.
Villaseñor, R., Kalaidzidis, Y. and Zerial, M. (2016). Signal processing by the endosomal system. *Curr. Opin. Cell Biol.* **39**, 53-60.
Wang, Y., Pennock, S. D., Chen, X., Kazlauskas, A. and Wang, Z. (2004). Platelet-derived growth factor receptor-mediated signal transduction from endosomes. *J. Biol. Chem.* **279**, 8038-8046.